Article

Deconstructing Protein Binding of Sulfonamides and Sulfonamide Analogues

Patrick L. Purder, Christian Meyners, Wisely Oki Sugiarto, Jürgen Kolos, Frank Löhr, Jakob Gebel, Thomas Nehls, Volker Dötsch, Frederik Lermyte, and Felix Hausch*

Cite This: *JACS Au* 2023, 3, 2478−2486

Read Online

ACCESS | Metrics & More | Article Recommendations | Supporting Information

ABSTRACT: Sulfonamides are one of the most important pharmacophores in medicinal chemistry, and sulfonamide analogues have gained substantial interest in recent years. However, the protein interactions of sulfonamides and especially of their analogues are underexplored. Using FKBP12 as a model system, we describe the synthesis of optically pure sulfenamide, sulfinamide, and sulfonimidamide analogues of a well characterized sulfonamide ligand. This allowed us to precisely determine the binding contributions of each sulfonamide oxygen atom and the consequences of nitrogen replacements. We also present high-resolution cocrystal structures of sulfonamide analogues buried in the pocket of a protein target. This revealed intimate contacts with the protein including an unprecedented hydrogen bond acceptor of sulfonimidamides. The use of sulfonamide analogues enabled new exit vectors that allowed remodeling of a subpocket in FKBP12. Our results illuminate the protein interaction potential of sulfonamides/sulfonamide analogues and will aid in their rational design.

KEYWORDS: sulfonamides, drug design, protein−ligand-interactions, sulfonimidamides, FKBP
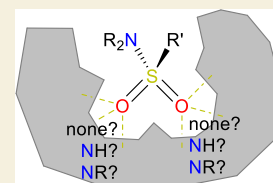
INTRODUCTION

Sulfonamides are indispensable in medicinal chemistry. Twenty-five percent of all FDA-approved new molecular entities from the first half of 2022 contained a sulfonamide motif.[a] Moreover, sulfonamide analogues, especially the =O to =NR exchanged sulfonimidamides (see Figure 1) and
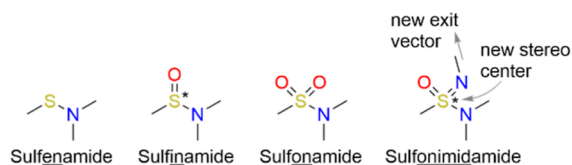

Figure 1. Structural motif of a sulfonamide and its analogues.

sulfoximines, have gained substantial momentum,[1−3] and the first successful examples show the potential of these modalities.[4−7] Notably, the new exit vector enabled by sulfonimidamides may open unprecedented opportunities for the structure-based design of sulfonamide analogues, but structurally well-documented examples for this are still lacking.

In line with the prevalence of sulfonamides, over 1000 cocrystal structures are available in the PDB harboring sulfonamide-containing ligands.[b] However, the contribution of the sulfonamide motif to affinity is usually poorly defined and little is known regarding the interaction energies resulting from the sulfonamide oxygen-protein contacts.

RESULTS AND DISCUSSION

The FK506-binding protein 12 (FKBP12) is a widely used model system for ligand−protein interaction studies that binds to sulfonamides as one of its preferred recognition motifs.[8−15] Notably, the sulfonamide oxygens are thought to be a key binding motif for these ligands and mimic the α-keto amide of FK506 (Supporting Information, Figure S5) and similarly engage in unusual but highly conserved CH⋯O=S interactions with the protein.[16,17] Taking advantage of this highly conserved binding mode, we set out to explore the interactions of sulfonamides and their derivatives with FKBP12.

Toward this goal, we used the bicyclic sulfonamide **1** (known as compound **16a** in Pomplun et al.[11] and compound **16** in Kolos et al.,[10] see Scheme 1 for the chemical structure) since it binds to FKBP12 with high affinity[10] and the binding mode of this compound class is well established.
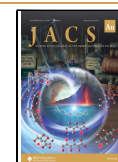
The synthesis of the sulfonamide analogues started with the known precursor **2**,[11] derived from the synthesis of sulfonamide-based FKBP ligands (Scheme 1). Here, amine **2** was coupled with freshly prepared sulfenyl chloride to give sulfenamide **3**. The activation of 3,5-dichlorothiophenol was
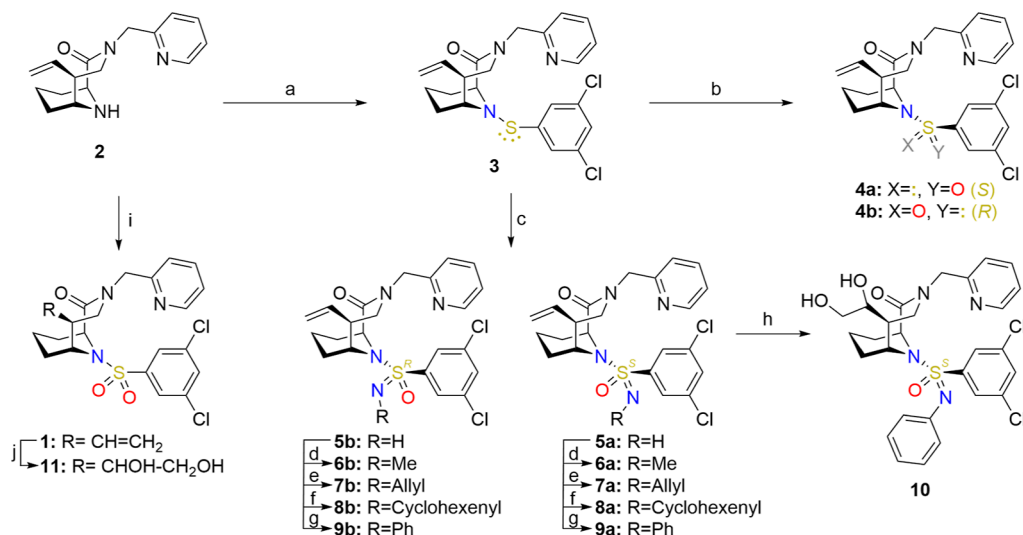
Scheme 1[a]

[a]Reagents and conditions: (a) 3,5-dichlorobenzenethiol, HOAc, SO₂Cl₂, −40 °C to rt, then **2**, DIPEA, MeCN, 19 h, rt, 55%; (b) KF, mCPBA, MeCN/H₂O 5:1, 30 min, 0 °C, then **3**, 5 h, 0 °C, 5% **4b** and 7% **4a** (separated diastereomers); (c) PhI(OAc)₂, AcONH₄, MeOH, 19 h, rt, 26% **5a** and 35% **5b** (separated diastereomers); (d) NaH, MeI, THF, 24 h, 0 °C to >rt, 82% **6a**, 64% **6b**; (e) NaH, allyl bromide, THF, 42 h, 0 °C to >rt, 100% **7a**, 81% **7b**; (f) NaH, 3-bromocyclohexene, 2–5 d 0 °C to >rt, 66% **8a**, 85% **8b**; (g) PhB(OH)₂, Cu(OAc)₂, TEA, MeCN, 18–42 h rt, 100% **9a**, 87% **9b**; (h) 2,6-lutidine, NMO, OsO₄, acetone/water (10:1), 4 d, rt, 62%; (i) 3,5-dichlorobenzenesulfonyl chloride, DIPEA, dry MeCN, 19 h, rt, 48%; and (j) 2,6-lutidine, NMO, OsO₄, acetone/water 7:1, 16 h, rt, 54%.

performed with sulfuryl chloride and acetic acid, as described by Martzel et al.[18] The aim was to form the respective sulfinyl chloride and after the reaction with **2** the respective sulfenamide. Surprisingly, the only product found in this reaction was sulfenamide **3**. The sulfenamide **3** was then oxidized to sulfinamides **4a/b**. To prevent overoxidation, KF/mCPBA was used as oxidizing agent, as described by Datta and Buglass.[19] The sulfinamides could be obtained as pure diastereomers by preparative HPLC. Oxidative imination of sulfenamide **3**, following the approach of Zenzola et al.,[20] provided sulfonimidamides **5a/b**, which were readily separable by silica gel column chromatograpy. The isolated sulfonimidamides were then alkylated with methyl iodide (**6a/b**), allyl bromide (**7a/b**), and 3-bromocyclohexene (**8a/b**). A Chan−Lam reaction with phenylboronic acid, as described by Battula et al.,[21] yielded products **9a/b**. Compounds **8a/b** were synthesized as respective mixtures of cyclohexenyl-C1-epimers, which were not preparatively separated.

The sulfinamides, N-unsubstituted sulfonimidamides, and substituted sulfonimidamides (methyl, allyl, cyclohexenyl, and phenyl substituted) could be obtained as stable and separated diastereomers arising from the chiral sulfur. The configurations of the sulfur atoms of the alkylated sulfonimidamides **6a/b** and **7a/b** could be determined via NOESY-NMR (Supporting Information, Figures S1 and S2), which also defined the configuration of the respective precursors **5a/b** and other derivatives thereof (**8a/b** and **9a/b**). The configurations of the sulfinamides **4a/b** were assigned indirectly by stereoselective conversion to **5a/b** (Supporting Information, Figure S3). Cocrystal structures later confirmed the assigned configurations (Figure 2 and S6−12).

The S-configured phenyl-substituted sulfonimidamide **9a** and the reference sulfonamide **1** were dihydroxylated at their respective vinyl groups in the C5 position of the core to give **10** and **11** to increase aqueous solubility, which was required for protein NMR studies (see below).

The binding affinities for FKBP12 of the sulfenamide, sulfinamide, and sulfonimidamide ligands were measured by a fluorescence polarization assay using sulfonamide **1** as a reference. For **1** and four analogues, we were also able to solve cocrystal structures with FKBP12 and the FK506-binding domain of FKBP51[22] at high resolutions (1.0−1.7 Å, Figure 2 and Supporting Information Figures S6−S12).[c]

Additional binding affinity data for three other human FKBPs and two FKBP-like proteins from human pathogens are given in Supporting Information, Table S1. The same trends can be observed as for FKBP12, within an affinity offset characteristic for each specific FKBP homologue. Solely the preference for the sulfinamide stereochemistry (**4a** and **4b**) changed from human FKBPs to FKBP-like proteins. This indicates that the findings obtained for FKBP12 are largely representative for the FKBP family.

All sulfonamide analogues bound weaker compared to the reference sulfonamide **1** (K_D = 2.6 nM). This was expected since the latter was highly optimized for FKBP12. The cocrystal structure of **1** in complex with FKBP12 revealed its interaction network (Figure 2A,B), confirming the expected binding mode.

The pipecolate core of **1** is buried in a hydrophobic pocket exactly like the pipecolate core of the natural ligand FK506 (see Supporting Information, Figure S5). **1** forms two hydrogen bonds with FKBP12 (amide-C=O⋯HN-Ile56 and pyridine-N⋯HO-Tyr82), one dipolar interaction [amide-C(=O)⋯HO-Tyr82], and one halogen-π-interaction (aryl-Cl⋯π-His87). In analogy to the carbonyl oxygens of FK506 (see Supporting Information, Figure S5), the sulfonamide oxygens form a network of S=O⋯HC interactions with aromatic chains of Tyr26, Phe36, Tyr82, and Phe99.

The availability of the sulfenamide (**3**), sulfonamide (**1**) and both sulfinamides (**4a/b**) allowed—for the first time—to dissect the energetic contributions of each sulfonamide oxygen atom to binding affinity (see Table 1 and Supporting Information, eq
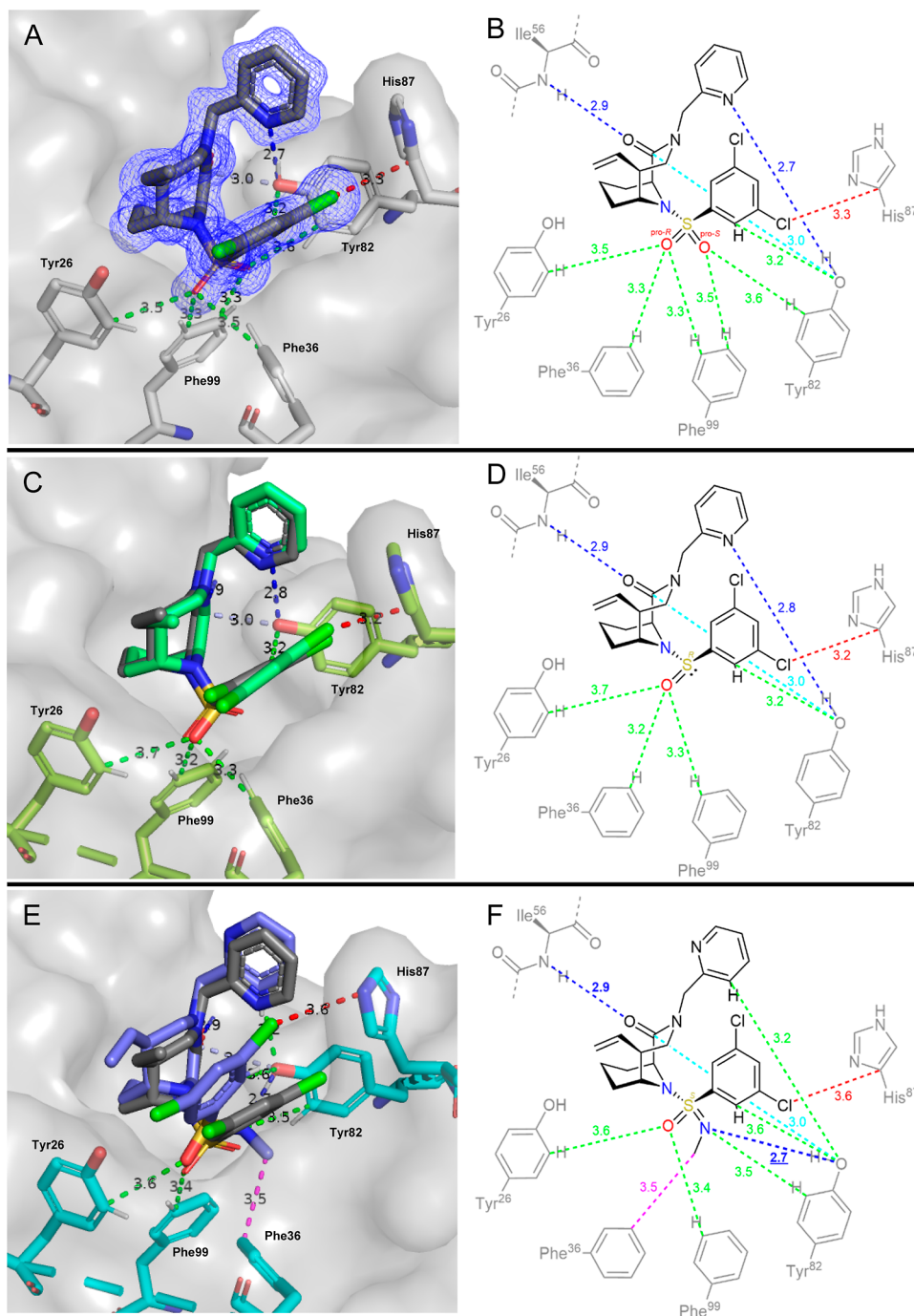
Figure 2. Cocrystal structure of bicyclic sulfonamides and analogues thereof. **1** [(A) PDB: 8CHL], **4b** [(C) PDB: 8CHM], and **6a** [(E) PDB: 8CHI] in complex with FKBP12. In (A,C), the binding pose of ligand **1** has been superimposed as gray sticks. 2D-interaction networks for these compounds are shown on the right (B,D,F). Hydrogen bonds are shown in blue, halogen-π-interactions are shown in red, CH···O/N interactions are shown in green, and other polar contacts are shown in light blue. Distances of dashed lines are given in Å. Electron density of the ligand **1** is shown as a blue mesh in part A. The distance of the sulfonimidamide methyl group of ligand **6a** to Phe36 is shown in pink.

S1).[24] Both oxygen atoms combined accounted for a binding energy of −13.1 kJ/mol. Surprisingly, the interactions of both oxygens were coupled, with the removal of the first oxygen ($\Delta\Delta G$ = 8.05−9.67 kJ/mol) being much more detrimental than the subsequent removal of the second oxygen ($\Delta\Delta G$ = 3.40−5.02 kJ/mol). This overproportional effect led to a 1.4-fold higher binding energy for the combined two oxygens than the sum of both oxygen atoms separately. In direct comparison, the *R*-configured sulfinamide **4b** was slightly preferred over the *S*-configured sulfinamide **4a**. This suggests

that the oxygen predicted to be in vicinity to Tyr26 contributes more to the overall binding energy than the oxygen predicted to be in vicinity to Tyr82. This orientation was confirmed by the cocrystal structures of **4b** (Figure 2C,D with FKBP12, Supporting Information, Figure S6 with FKBP51FK1), which also showed that the overall binding mode is only minimally perturbed by the removal of the pro-*S* oxygen and that all protein interactions typical for this class of ligands are maintained.

Table 1. Binding Affinities of all Sulfonamide Analogues for FKBP12, Measured in a Competitive Fluorescence Polarization Assay[23][a]

Compound	Structure C5 substituent	Sulfur motif	K_D for FKBP12 in nM	Compound	Structure C5 substituent	Sulfur motif	K_D for FKBP12 in nM
1[a]	Vinyl		2.6 ±0.2	8a	Vinyl		490 ±57
3	Vinyl		509 ±152				
4a	Vinyl		129 ±19	8b	Vinyl		577 ±85
4b[ab]	Vinyl		67 ±5				
5a[ab]	Vinyl		360 ±27	9a	Vinyl		658 ±160
5b[ab]	Vinyl		283 ±24				
6a[ab]	Vinyl		1,390 ±190	9b	Vinyl		>40,000
6b	Vinyl		1,160 ±120	11	1,2-Dihydroxy-ethyl		0.6 ±0.1
7a	Vinyl		1,570 ±180	10	1,2-Dihydroxy-ethyl		8,770 ±610
7b	Vinyl		912 ±108				

[a]Core = (1S,5S,6R)-2-oxo-3-(pyirin-2-ylmethyl)-3,10-diazabicyclo[4.3.1]decan-10-yl, Ar = 3,5-dichlorophenyl (corresponds to 2, see Scheme 1). [b]Cocrystal structure with FKBP12 solved. [c]Cocrystal structure with FKBP51FK1 solved.

The interaction network of 4b is equivalent to the interactions of sulfonamide 1, apart from the missing oxygen. The remaining sulfinamide oxygen forms the same S=O···HC interactions with Tyr26, Phe36, and Phe99 as observed for 1. The protein did not adapt to the gap created by the removed oxygen atom in vicinity to Tyr82. The missing S=O···HC interactions of said oxygen obviously account for the sulfinamide's lower binding affinity.

With the contributions of each sulfonamide oxygen defined, we explored the effect of stereospecific substitution by nitrogens. Replacing an oxygen with an unsubstituted nitrogen was more detrimental (K_D = 360 and 283 nM) than removing an oxygen altogether, for either configuration. Cocrystal structures for both diastereomers (5a/b) revealed an overall conserved binding mode (Supporting Information, Figures S7−S10). The distances of the S=O···HC and S=NH···HC

interactions did not significantly deviate from the corresponding S=O···HC distances in the sulfonamide **1**, and the binding modes offer enough space to accommodate the additional hydrogen. For the diastereomer **5b**, the dichlorophenyl ring adopts different poses compared to the sulfonamide **1** (Supporting Information, Figure S9E,G), likely reflecting an attempt to ameliorate unfavorable interactions of the buried free NH of the sulfonimidamide.

Taken together, the crystallographic analysis suggests that the desolvation cost for an unsubstituted S(=O)=NH in the free sulfonimidamides (**5a/b**) is much higher compared to the SO$_2$ in sulfonamides and in this particular case is poorly compensated by new interactions with FKBP12.

To reduce the desolvation cost, we methylated the sulfonimidamides, as in **6a/b**. However, this reduced the affinity even further (K_D = 1390 and 1160 nM). The cocrystal structure of **6a** showed that this can be attributed to a steric clash, which is reflected by a twist of the ligand's dichlorophenyl ring (Supporting Information, Figures S11 and S12).

Surprisingly, in the complex of **6a** with FKBP12, we observed a very short contact of the sulfonimidamide nitrogen [S(=O)=**N**Me] to the hydroxyl group of Tyr82 (2.7 Å, Figure 2E,F and Supporting Information Figure S11A). This is substantially below van-der-Waals distance. The geometry is consistent with a hydrogen bond between S(=O)=**N**Me and **HO**-Tyr82. To the best of our knowledge, this is the first direct experimental evidence that sulfonimidamides can act as hydrogen bond acceptors in protein complexes. It should be noted, however, that the results obtained by cocrystallography represent snapshots and the interaction pattern might be more dynamic in solution, including a competition between hydrogen bonding to S(=O)=**N**Me or the pyridine-N.

A key prospect of sulfonimidamides compared with sulfonamides is the additional exit vector available in the former. To explore this option, we further increased the size of the sulfonimidamide substituent as in **7a/b** (allyl), **8a/b** (cyclohexenyl), and **9a/b** (phenyl). Surprisingly, this did not further compromise affinity, although all these modifications were expected to severely clash with the protein. With the exception of the R-configured phenyl-substituted sulfonimidamide **9b** (K_D > 40 μM), the affinities actually improved for the larger substituents, which is difficult to reconcile with the previously observed canonical binding mode.

To clarify this, we analyzed the complexes by native MS and protein NMR experiments. For solubility reasons, we used the dihydroxylated analogues **11** and **10** since this modification is known to maintain the canonical binding mode for sulfonamide ligands.[15]

Native mass spectrometry further confirmed the direct binding of **11** and **10** to FKBP12. Complementary ion mobility measurements indicated no major conformational change for either ligand (Supporting Information, Figure S13). The **11**-FKBP12 complex was found to be more stable toward collisional activation than the **10**-FKBP12 complex (Supporting Information, Figure S14), in line with the higher affinity of the former. HDX analyses revealed that similar to the sulfonamide ligands, **10** induced a more shielded conformation in parts of FKBP12. In contrast, some regions such as the 30s loop preceding F36 showed enhanced accessibility, similar to the F36-displacing FKBP ligand SAFit1[25,26] (Supporting Information, Figure S15).

When investigating the **11**- and **10**-FKBP12 complexes by NMR spectroscopy (Supporting Information, Figures S16 and S17), four sets of signals were particularly informative: (i) NOESY experiments showed the pyridines of **10** and **11** to be in close proximity to the Tyr82 side chain (Figure 3 and
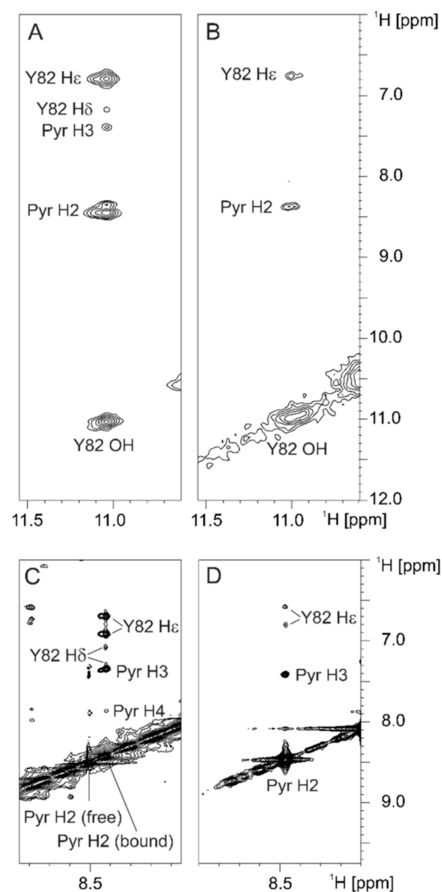

Figure 3. 2D NOESY spectra of [u-^{13}C/^{15}N]-labeled FKBP12 with **11** (A,C) and **10** (B,D) recorded at 700 MHz, showing the Tyr82 side chain being close to the ligand pyridine rings. Spectra in panels A and B were acquired at a sample temperature of 272 K using 0.5 mM FKBP sample in 25 mM phosphate buffer, pH 7, containing 5% D$_2$O with a twofold excess of inhibitors. Samples for recording spectra in panels (C,D) contained 0.1 mM of [u-^{13}C/^{15}N]-FKBP12 + 0.36 mM **11** and 0.04 mM of [u-^{13}C/^{15}N]-FKBP12 + 0.2 mM **10**, respectively, in 95–98% D$_2$O. The latter spectra were recorded at a temperature of 298 K without ^{13}C decoupling such that peaks involving the labeled protein exhibit a large doublet splitting due to $^1J_{CH}$, whereas inhibitor peaks do not.

Supporting Information, Figure S17), consistent with a key hydrogen bond (see Figure 2). (ii) The amide signal of the indole side chain of Trp59 was shifted downfield in the presence of **10** and **11** (Supporting Information, Figure S16C), which is highly characteristic for Trp59 being pushed deeper into the binding pocket. (iii) The HSQC signals of Ile56(NH) were strongly shifted by either **10** and **11** (Supporting Information, Figure S16D). This is consistent with a hydrogen bond to the carbonyl group of **10** and **11**, which is a key interaction of FKBP ligands, including all structures presented in this work (Figure 2). (iv) The only HSQC signal missing for the **10**-FKBP12 complex was for Phe36 and Tyr82 (Supporting Information, Figure S16E), which are predicted to be close to the N-substitution site of **10** (Figure 2E,F).

Collectively, these data show that **10** binds with the overall typical FKBP ligand binding mode where the *N*-phenyl substituent of the sulfonimidamide is accommodated by adaptions of F36 and Y82.

CONCLUSIONS

Our set of optically pure sulfenamide, sulfinamide, and sulfonimidamide analogues, together with the experimentally confirmed highly conserved binding mode, allowed us to precisely investigate the binding contributions of each sulfonamide oxygen as well as nitrogen substitutions thereof. For one ligand (**6a**), we provide clear evidence that sulfonimidamide nitrogen atoms can act as hydrogen bond acceptors in protein complexes. Finally, we show that substituents on sulfonimidamides enable new ways to engage proteins, which, in this case, revealed a dynamic rearrangement of a subpocket in FKBP12. Taken together, our findings provide a better understanding of how sulfonamides and sulfonimidamide analogues interact with proteins, which will help in the rational design of sulfon(imid)amide-containing drugs.

METHODS

FP Assay

For most pipetting steps of the FP Assay, a Beckman Coulter FX[P] Laboratory Automation Workstation was used. As tracer, the fluorescent ligand **16g** developed by Pomplun et al.[11] was used. The compound was diluted in a 1:2 serial dilution in DMSO and then mixed with protein and tracer in buffer (20 mM HEPES, pH 8, 0.002% v/v Triton X-100, 150 mM NaCl) in a black, nonbinding 384-well plate, and then incubated in the dark for 30 min. Polarization was measured on a Tecan Spark at room temperature with an excitation wavelength of 535 nm and an emission wavelength of 595 nm. The assay was performed in triplicates. The competition curves were visualized using GraphPad Prism 6.0, K_D values were calculated from the fitting according to Kozany et al.[23] The final parameters are listed in Supporting Information, Table S2.

Crystallization

Complexes were prepared by mixing FKBP12 C22 V at 25.6 mg/mL (**5a**, **5b**, and **6a**) or 31.7 mg/mL (**1** and **4b**) or FKBP51FK1 A19T, C103A, C107I (14−140) at 28 mg/mL formulated in 20 mM HEPES-NaOH pH 8.0 and 20 mM NaCl with a slight molar excess of ligand previously dissolved at 20 mM in DMSO. For complexes of FKBP12 and **1** and **4b** crystallization was performed at room temperature using the sitting drop vapor-diffusion method, equilibrating mixtures of 1 μL of protein complex and 1 μL of reservoir against 30 μL of reservoir solution. For **1**, crystals were obtained from reservoir solutions containing 2.2 M ammonium sulfate and 0.2 M cadmium sulfate. For **4b**, crystals were obtained from reservoir solutions containing 2.1 M ammonium sulfate, 0.2 M cadmium chloride, and 0.1 M HEPES-NaOH pH 7.5. For complexes of FKBP12 and **5a**, **5b**, and **6a** crystallization was performed at room temperature using the hanging drop vapor-diffusion method, equilibrating mixtures of 1 μL of protein complex and 1 μL of reservoir against 500 μL of reservoir solution. Crystals were obtained from reservoir solutions containing 1.32−1.4 M Na/K tartrate, 0.2 M ammonium citrate, and 0.1 M MES pH 6.5. Crystals were fished, cryoprotected with LV CryoOil (Jena Bioscience), and flash frozen in liquid nitrogen. For complexes with FKBP51FK1 crystallization was performed at room temperature using the hanging drop vapor-diffusion method, equilibrating mixtures of 1 μL protein complex and 1 μL reservoir against 500 μL reservoir solution. Crystals were obtained from reservoir solutions containing 30−32% PEG-3350, 0.2 M NH₄-acetate, and 0.1 M HEPES-NaOH pH 7.5. Crystals were fished and flash frozen in liquid nitrogen.

Structure Solution and Refinement

The crystallographic experiments were performed on the BL14.1 and BL14.2 beamlines at the Helmholtz-Zentrum BESSY II synchrotron, Berlin, Germany.[27] Diffraction data were integrated with XDS and further processed with the implemented programs of the CCP4i and CCP4i2 interface.[28−31] The data reduction was conducted with Aimless.[31−33] Crystal structures were solved by molecular replacement using Phaser.[34] Iterative model improvement and refinement were performed with Coot and Refmac5.[35−40] The dictionaries for the compounds were generated wit PRODRG implemented in CCP4i.[41] Residues facing solvent channels without detectable side chain density were truncated. Refinement data are shown in Supporting Information, Tables S3−S5

Ion Mobility Mass Spectroscopy

An FKBP12 stock solution of 44 mg/mL in 20 mM sodium chloride and 20 mM HEPES was rebuffered. For the rebuffering, a 3k Amicon Ultra Centrifugal Filter from Merck was first precleared with 500 μL of a 200 mM ammonium acetate buffer (pH 7, LC−MS grade) at 14g for 30 min. The ammonium acetate buffer is a native volatile buffer.[42] Then, 100 μL of protein stock solution was added, filled up to 500 μL with ammonium acetate buffer, and rebuffered at 14g for 30 min. The previous step was performed five times in total. The rebuffered protein solution was then diluted with an ammonium acetate buffer to an initial concentration of 44 mg/mL (∼3.7 mM). Of the ligands, a stock solution of 20 mM in DSMO was diluted to 2 mM with DMSO. For the final solution, 0.5 μL of the protein dilution and 1 μL of ligand dilution or DMSO (for Apo-FKBP12) were combined and filled to 50 μL with 200 mM ammonium acetate buffer. This resulted in a final concentration of a 40 μM protein−ligand solution.

All sample solutions were measured using direct-infusion nanoESI on a Synapt G2-S instrument from Waters. Capillary voltage was between 1 and 2 kV; sampling cone voltage was at 10 V, and source temperature was 30 °C. For the ion mobility measurements and collision-induced unfolding experiments, a Trap DC Bias of 35 V was used in combination with an IMS Wave Velocity of 1000 m/s. The drift gas was nitrogen, and the collision gas was argon. The collision-induced unfolding experiments started at a trap collision energy of 4 V, continuing at 10 V in 5 V steps to 70 V and then in 10 V steps to a maximum of 160 V. The evaluation of collision-induced unfolding experiments was done with CIUSuite 2.[43] CCS calibration was performed with ubiquitin from bovine[44] (charge state 4+ with 949 Å²), cytochrome c from horse[44] (charge state 7+ with 1536 Å²) and holomyoglobin from horse[44] (charge state 7+ with 1863 Å², 9+ with 2085 Å²). A logarithmic regression model was chosen for calibration.[45] Regression coefficient R^2 was 0.98964.

HDX

An FKBP12 stock solution of 4.24 mM in 20 mM sodium chloride and 20 mM HEPES was diluted with 200 mM ammonium acetate buffer (pH 7, LC−MS grade) to a concentration of 424 μM. The ligand stock solutions of 20 mM in DMSO were diluted to a concentration of 2.4 mM with DMSO. For the final solution, 9.44 μL of protein dilution and 2 μL of ligand dilution or DMSO (for Apo-FKBP12) were combined and filled up to 400 μL with 200 mM ammonium acetate buffer.

Labeling and measurements were performed by using an HDX setup from Waters. This includes a PAL RTC Autosampler from LEAP Technologies, a UHPLC with μBinary Pump and Auxiliary Pump from Waters, the HDX Manager of separate column ovens for the pepsin column and analytical column from Waters, and a Synapt XS from Waters. Protein solutions were stored in the quench tray at 1 °C under nitrogen. Three μL of protein solution was injected into the label vial. Then, 57 μL of label buffer (pH 7, 5 mM K₂HPO₄ and 5 mM KH₂PO₄ in D₂O) or equilibration buffer (pH 7, 5 mM K₂HPO₄ and 5 mM KH₂PO₄ in H₂O) was added and allowed to react for the set time at 20 °C. A 50 μL portion of the reaction solution was transferred to the quench vial in the quench tray. In this process, 50 μL of the quench buffer (pH 2.3, 50 mM K₂HPO₄ and 50 mM

KH$_2$PO$_4$ in H$_2$O) had already been placed at 1 °C at least 30 min earlier.

50 μL of quenched sample was injected and flowed for 3 min with a flow of 200 μL/min with 0.2% formic acid in H$_2$O over the BEH pepsin column, 5 μm, 30 × 2.1 mm, 300 Å from Waters at 20 °C to the trap column ACQUITY UPLC BEH C18 VanGuard Precolumn, 1.7 μm, 5 × 2.1 mm, 130 Å from Waters at 1 °C. Thereafter, it started a gradient at 95% eluent A (0.2% formic acid inside H$_2$O) and 5% eluent B (acetonitrile with 0.2% formic acid) over the trap column to the analytical column ACQUITY UPLC BEH C18, 1.7 μm, 150 × 1 mm, 130 Å from Waters at 1 °C. The gradient continued to 40% eluent A and 60% eluent B over 10 min and then to 100% eluent B over 3 min which was held for 2 min, all with a flow of 45 μL/min. ESI was used as ionization and as MS method, an HDMSe with nitrogen as the collision gas was used. As LockSpray for recalibration, a solution of 2 ng/μL leucine enkephalin inside 50:50 acetonitrile/water with 0.1% formic acid was infused.

The labeled protein samples were measured n = 5 times for each time point at 1, 10, and 100 min, and the protein samples with equilibration buffer with time point 0 min were measured with n = 2 for each protein conformation. All measurements with a time point of 0 min were combined as reference. The evaluation was performed using ProteinLynx Global Server and DynamX, both software from Waters. Based on the peptide fragmentation pattern, a score threshold of 7.75 was chosen for the identified peptides and an intensity threshold of 10,000. This resulted in a sequence coverage of 100% with 30 peptides, of which the most important ones are presented.

Nuclear Magnetic Resonance

For each FKBP-inhibitor complex, two different samples were employed to collect NOESY data. The first set of samples contained 1 mM inhibitor and 0.5 mM [u-^{13}C/^{15}N]-labeled FKBP in 25 mM phosphate buffer at pH7 with 5% D$_2$O and 5% DMSO and had volumes of 0.6 mL in standard 5 mm NMR tubes ("H$_2$O samples"). For the second set, stock solutions of inhibitors 10 and 11 in DMSO-d_6 were dissolved in 99% D$_2$O and titrated with [u-^{13}C/^{15}N]-labeled FKBP in a nondeuterated phosphate buffer. Final concentrations were 0.2 mM 10 with 0.04 mM FKBP and 0.36 mM 11 with 0.1 mM FKBP, respectively, with sample volumes of 0.3 mL placed in 5 mm Shigemi tubes ("D$_2$O samples").

Spectra were recorded at a Bruker AvIII HD 700 MHz spectrometer, equipped with a cryogenic ^{1}H{^{31}P/^{13}C/^{15}N} QCI probe and Bruker AvIII HD 800 and AvIII 950 MHz spectrometers, both equipped with cryogenic ^{1}H{^{13}C/^{15}N} TCI probes.

For detection of NOEs involving the FKBP Tyr82 OH group, 2D NOESY spectra were recorded with the H$_2$O samples at a temperature of 272 K. To avoid saturation of the exchanging hydroxyl protons, a 1−1 echo water suppression scheme was employed with the excitation maximum adjusted to 12 ppm, whereas the strong DMSO signal was suppressed by presaturation. Carbon-13 decoupling was applied in the F_1 dimension. Mixing times were 30 ms for the complex with 10 and 50 ms for the complex with 11. The same set of samples was employed for the detection of NOEs with Tyr82 C$^\epsilon$H protons, but measurements were carried out at 298 K. A 3D F_1-^{13}C/^{15}N-filtered NOESY-[^{13}C,^{1}H]-HMQC (100 ms mixing time) optimized for aromatic CH groups was recorded for the complex with 11. For sensitivity reasons, only a 2D ^{1}H−^{1}H plane from a simple (nonfiltered) aromatic 3D NOESY-[^{13}C,^{1}H]-HMQC (50 ms mixing time) was recorded for the complex with 10. Here, ^{13}C decoupling was omitted in the indirect ^{1}H dimension to enable the identification of intermolecular NOEs from the lack of a $^1J_{CH}$ splitting of the cross peaks. Standard 2D NOESY spectra (10: 100 ms mixing time; 11: 70 ms mixing time) were recorded with the D$_2$O-samples to allow for a clean detection of inhibitor peaks without a background of FKBP amide signals. The residual water signal was suppressed using excitation sculpting. Again, no ^{13}C decoupling was applied, such that intermolecular NOEs involving the ^{13}C labeled FKBP can be identified by the $^1J_{CH}$ splitting (ca. 160 Hz in the case of Tyr H$^\epsilon$).

NMR Titration experiments were recorded on the spectrometers described above. Sample temperatures were either 298 K (Supporting Information, Figure 16A) or 313 K (Supporting Information, Figure 16B). 15N-BEST-TROSY spectra were recorded with 384 points in t1 and 40 ppm spectral width. Protein starting concentration was 50 μM and titration steps were conducted by the addition of the corresponding volume of compounds (20 mM stock concentration).

■ ASSOCIATED CONTENT

Ⓢ Supporting Information

The Supporting Information is available free of charge at https://pubs.acs.org/doi/10.1021/jacsau.3c00241.

NMR assignments of sulfonimidamide diastereomers, binding affinities of all sulfonamide analogues, cocrystal structures, ion mobility mass spectra, collision-induced unfolding and dissociation results, HDX measurements, NOESY spectra of FKBP12 complexes, parameters of the performed FP assays, refinement data of the cocrystal structures, synthetic procedures, and ^{1}H- and ^{13}C NMR spectra (PDF)

■ AUTHOR INFORMATION

Corresponding Author

Felix Hausch − *Department of Organic Chemistry and Biochemistry, Clemens-Schöpf-Institute, Technical University Darmstadt, 64287 Darmstadt, Germany; Centre for Synthetic Biology, Technical University of Darmstadt, 64287 Darmstadt, Germany;* ⓘ orcid.org/0000-0002-3710-8838; Email: felix.hausch@tu-darmstadt.de

Authors

Patrick L. Purder − *Department of Organic Chemistry and Biochemistry, Clemens-Schöpf-Institute, Technical University Darmstadt, 64287 Darmstadt, Germany*

Christian Meyners − *Department of Organic Chemistry and Biochemistry, Clemens-Schöpf-Institute, Technical University Darmstadt, 64287 Darmstadt, Germany*

Wisely Oki Sugiarto − *Department of Organic Chemistry and Biochemistry, Clemens-Schöpf-Institute, Technical University Darmstadt, 64287 Darmstadt, Germany*

Jürgen Kolos − *Department of Organic Chemistry and Biochemistry, Clemens-Schöpf-Institute, Technical University Darmstadt, 64287 Darmstadt, Germany*

Frank Löhr − *Institute of Biophysical Chemistry and Center for Biomolecular Magnetic Resonance, Goethe University, 60438 Frankfurt am Main, Germany;* ⓘ orcid.org/0000-0001-6399-9497

Jakob Gebel − *Institute of Biophysical Chemistry and Center for Biomolecular Magnetic Resonance, Goethe University, 60438 Frankfurt am Main, Germany*

Thomas Nehls − *Department of Organic Chemistry and Biochemistry, Clemens-Schöpf-Institute, Technical University Darmstadt, 64287 Darmstadt, Germany*

Volker Dötsch − *Institute of Biophysical Chemistry and Center for Biomolecular Magnetic Resonance, Goethe University, 60438 Frankfurt am Main, Germany;* ⓘ orcid.org/0000-0001-5720-212X

Frederik Lermyte − *Department of Organic Chemistry and Biochemistry, Clemens-Schöpf-Institute, Technical University Darmstadt, 64287 Darmstadt, Germany*

Complete contact information is available at:
https://pubs.acs.org/10.1021/jacsau.3c00241

Author Contributions

The manuscript was written through contributions of all authors. All authors have given approval to the final version of the manuscript. CRediT: **Thomas Nehls** investigation, methodology.

Funding

Notes

The authors declare no competing financial interest.

■ ACKNOWLEDGMENTS

■ ADDITIONAL NOTES

[a]www.accessdata.fda.gov/scripts/cder/daf/index.cfm?event=reportsSearch.process&rptName=2&reportSelectMonth=6&reportSelectYear=2022&nav#navigation.
[b]https://www.rcsb.org/ → advanced search → Chemical Similarity → Query Type "Descriptor"; Descriptor Type "SMILES"; Match Type "Substructure (including Stereoisomers)" → Search "CS(N)(=O)=O".
[c]To the best of our knowledge, the only PDB entries for sulfonamide analogues are 2CI1, which harbors a N-thiosulfinamide, which is generated enzymatically in situ from a S-nitroso-thiol, and 7JTC and 7T36, where the geometry of the ligands needs to be confirmed and the associated publication remains to be published.

■ REFERENCES

(1) Frings, M.; Bolm, C.; Blum, A.; Gnamm, C. Sulfoximines from a Medicinal Chemist's Perspective: Physicochemical and in vitro Parameters Relevant for Drug Discovery. *Eur. J. Med. Chem.* **2017**, *126*, 225−245.

(2) Chinthakindi, P. K.; Naicker, T.; Thota, N.; Govender, T.; Kruger, H. G.; Arvidsson, P. I. Sulfonimidamides in Medicinal and Agricultural Chemistry. *Angew. Chem., Int. Ed. Engl.* **2017**, *56* (15), 4100−4109.

(3) Lücking, U. Sulfoximines: a neglected opportunity in medicinal chemistry. *Angew. Chem., Int. Ed. Engl.* **2013**, *52* (36), 9399−9408.

(4) Davies, T. Q.; Hall, A.; Willis, M. C. One-Pot, Three-Component Sulfonimidamide Synthesis Exploiting the Sulfinylamine Reagent N-Sulfinyltritylamine, TrNSO. *Angew. Chem., Int. Ed. Engl.* **2017**, *56* (47), 14937−14941.

(5) Steinkamp, A.-D.; Schmitt, L.; Chen, X.; Fietkau, K.; Heise, R.; Baron, J. M.; Bolm, C. Synthesis of a Sulfonimidamide-Based Analog of Tasisulam and Its Biological Evaluation in the Melanoma Cell Lines SKMel23 and A375. *Skin Pharmacol. Physiol.* **2016**, *29* (6), 281−290.

(6) Thota, N.; Makam, P.; Rajbongshi, K. K.; Nagiah, S.; Abdul, N. S.; Chuturgoon, A. A.; Kaushik, A.; Lamichhane, G.; Somboro, A. M.; Kruger, H. G.; Govender, T.; Naicker, T.; Arvidsson, P. I. N-Trifluoromethylthiolated Sulfonimidamides and Sulfoximines: Antimicrobial, Anti-mycobacterial, and Cytotoxic Activity. *ACS Med. Chem. Lett.* **2019**, *10* (10), 1457−1461.

(7) Lücking, U. New Opportunities for the Utilization of the Sulfoximine Group in Medicinal Chemistry from the Drug Designer's Perspective. *Chem.—Eur. J.* **2022**, *28* (56), No. e202201993.

(8) Bischoff, M.; Sippel, C.; Bracher, A.; Hausch, F. Stereoselective construction of the 5-hydroxy diazabicyclo4.3.1decane-2-one scaffold, a privileged motif for FK506-binding proteins. *Org. Lett.* **2014**, *16* (20), 5254−5257.

(9) Gopalakrishnan, R.; Kozany, C.; Wang, Y.; Schneider, S.; Hoogeland, B.; Bracher, A.; Hausch, F. Exploration of pipecolate sulfonamides as binders of the FK506-binding proteins 51 and 52. *J. Med. Chem.* **2012**, *55* (9), 4123−4131.

(10) Kolos, J. M.; Pomplun, S.; Jung, S.; Rieß, B.; Purder, P. L.; Voll, A. M.; Merz, S.; Gnatzy, M.; Geiger, T. M.; Quist-Løkken, I.; Jatzlau, J.; Knaus, P.; Holien, T.; Bracher, A.; Meyners, C.; Czodrowski, P.; Krewald, V.; Hausch, F. Picomolar FKBP inhibitors enabled by a single water-displacing methyl group in bicyclic 4.3.1 aza-amides. *Chem. Sci.* **2021**, *12* (44), 14758−14765.

(11) Pomplun, S.; Sippel, C.; Hähle, A.; Tay, D.; Shima, K.; Klages, A.; Ünal, C. M.; Rieß, B.; Toh, H. T.; Hansen, G.; Yoon, H. S.; Bracher, A.; Preiser, P.; Rupp, J.; Steinert, M.; Hausch, F. Chemogenomic Profiling of Human and Microbial FK506-Binding Proteins. *J. Med. Chem.* **2018**, *61* (8), 3660−3673.

(12) Wang, Y.; Kirschner, A.; Fabian, A.-K.; Gopalakrishnan, R.; Kress, C.; Hoogeland, B.; Koch, U.; Kozany, C.; Bracher, A.; Hausch, F. Increasing the efficiency of ligands for FK506-binding protein 51 by conformational control. *J. Med. Chem.* **2013**, *56* (10), 3922−3935.

(13) Sun, F.; Li, P.; Ding, Y.; Wang, L.; Bartlam, M.; Shu, C.; Shen, B.; Jiang, H.; Li, S.; Rao, Z. Design and Structure-Based Study of New Potential FKBP12 Inhibitors. *Biophys. J.* **2003**, *85* (5), 3194−3201.

(14) Guo, C.; Augelli, S. C. E.; Barta, N. S.; Bender, S. L.; Bigge, C. F.; Caprathe, B. W.; Chatterjee, A.; Deal, J.; Dong, L.; Fay, L. K.; Hou, X.; Hudack, R. A., JR.; Warner, L. C. Heterobicycles fkbp-Ligands. WO 2002089806 A1, 2002.

(15) Pomplun, S.; Wang, Y.; Kirschner, A.; Kozany, C.; Bracher, A.; Hausch, F. Rational design and asymmetric synthesis of potent and neurotrophic ligands for FK506-binding proteins (FKBPs). *Angew. Chem., Int. Ed. Engl.* **2015**, *54* (1), 345−348.

(16) van Duyne, G. D.; Standaert, R. F.; Karplus, P. A.; Schreiber, S. L.; Clardy, J. Atomic structure of FKBP-FK506, an immunophilin-immunosuppressant complex. *Science* **1991**, *252* (5007), 839−842.

(17) van Duyne, G. D.; Standaert, R. F.; Karplus, P. A.; Schreiber, S. L.; Clardy, J. Atomic structures of the human immunophilin FKBP-12 complexes with FK506 and rapamycin. *J. Mol. Biol.* **1993**, *229* (1), 105−124.

(18) Martzel, T.; Lohier, J.-F.; Gaumont, A.-C.; Brière, J. F.; Perrio, S. Sulfinate-Organocatalyzed (3 + 2) Annulation Reaction of Propargyl or Allenyl Sulfones with Activated Imines. *Eur. J. Org. Chem.* **2018**, *2018* (36), 5069−5073.

(19) Datta, M.; Buglass, A. J. Fast and Efficient Synthesis of Sulfinamides by the Oxidation of Sulfenamides Using Potassium Fluoride and m -Chloroperoxybenzoic Acid. *Synth. Commun.* **2012**, *42* (12), 1760−1769.

(20) Zenzola, M.; Doran, R.; Degennaro, L.; Luisi, R.; Bull, J. A. Transfer of Electrophilic NH Using Convenient Sources of Ammonia: Direct Synthesis of NH Sulfoximines from Sulfoxides. *Angew. Chem., Int. Ed. Engl.* **2016**, *55* (25), 7203−7207.

(21) Battula, S.; Subbareddy, G. V.; Chakravarthy, I. E. A mild and efficient copper-catalyzed N-arylation of unprotected sulfonimidamides using boronic acids. *Tetrahedron Lett.* **2014**, *55* (2), 517−520.

(22) Bracher, A.; Kozany, C.; Thost, A. K.; Hausch, F. Structural characterization of the PPIase domain of FKBP51, a cochaperone of human Hsp90. *Acta Crystallogr., Sect. D: Biol. Crystallogr.* **2011**, *67* (6), 549−559.

(23) Kozany, C.; März, A.; Kress, C.; Hausch, F. Fluorescent probes to characterise FK506-binding proteins. *ChemBioChem* **2009**, *10* (8), 1402−1410.

(24) Du, X.; Li, Y.; Xia, Y.-L.; Ai, S.-M.; Liang, J.; Sang, P.; Ji, X.-L.; Liu, S.-Q. Insights into Protein-Ligand Interactions: Mechanisms, Models, and Methods. *Int. J. Math. Stat.* **2016**, *17* (2), 144.

(25) Gaali, S.; Kirschner, A.; Cuboni, S.; Hartmann, J.; Kozany, C.; Balsevich, G.; Namendorf, C.; Fernandez-Vizarra, P.; Sippel, C.; Zannas, A. S.; Draenert, R.; Binder, E. B.; Almeida, O. F. X.; Rühter, G.; Uhr, M.; Schmidt, M. V.; Touma, C.; Bracher, A.; Hausch, F. Selective inhibitors of the FK506-binding protein 51 by induced fit. *Nat. Chem. Biol.* **2015**, *11* (1), 33−37.

(26) Jagtap, P. K. A.; Asami, S.; Sippel, C.; Kaila, V. R. I.; Hausch, F.; Sattler, M. Selective Inhibitors of FKBP51 Employ Conformational Selection of Dynamic Invisible States. *Angew. Chem., Int. Ed. Engl.* **2019**, *58* (28), 9429−9433.

(27) Gerlach, M.; Mueller, U.; Weiss, M. S. The MX Beamlines BL14.1−3 at BESSY II. *JLSRF* **2016**, *2*, A47 DOI: 10.17815/jlsrf-2-64.

(28) Collaborative Computational Project, Number 4. The CCP4 suite: programs for protein crystallography. *Acta Crystallogr., Sect. D: Biol. Crystallogr.* **1994**, *50* (5), 760−763.

(29) Potterton, E.; Briggs, P.; Turkenburg, M.; Dodson, E. A graphical user interface to the CCP4 program suite. *Acta Crystallogr., Sect. D: Biol. Crystallogr.* **2003**, *59* (7), 1131−1137.

(30) Winn, M. D.; Ballard, C. C.; Cowtan, K. D.; Dodson, E. J.; Emsley, P.; Evans, P. R.; Keegan, R. M.; Krissinel, E. B.; Leslie, A. G. W.; McCoy, A.; McNicholas, S. J.; Murshudov, G. N.; Pannu, N. S.; Potterton, E. A.; Powell, H. R.; Read, R. J.; Vagin, A.; Wilson, K. S. Overview of the CCP4 suite and current developments. *Acta Crystallogr., Sect. D: Biol. Crystallogr.* **2011**, *67* (4), 235−242.

(31) Potterton, L.; Agirre, J.; Ballard, C.; Cowtan, K.; Dodson, E.; Evans, P. R.; Jenkins, H. T.; Keegan, R.; Krissinel, E.; Stevenson, K.; Lebedev, A.; McNicholas, S. J.; Nicholls, R. A.; Noble, M.; Pannu, N. S.; Roth, C.; Sheldrick, G.; Skubak, P.; Turkenburg, J.; Uski, V.; von Delft, F.; Waterman, D.; Wilson, K.; Winn, M.; Wojdyr, M. CCP4i2: the new graphical user interface to the CCP4 program suite. *Acta Crystallogr., Sect. D: Struct. Biol.* **2018**, *74* (2), 68−84.

(32) Evans, P. R. An introduction to data reduction: space-group determination, scaling and intensity statistics. *Acta Crystallogr., Sect. D: Biol. Crystallogr.* **2011**, *67* (4), 282−292.

(33) Evans, P. R.; Murshudov, G. N. How good are my data and what is the resolution? *Acta Crystallogr., Sect. D: Biol. Crystallogr.* **2013**, *69* (7), 1204−1214.

(34) McCoy, A. J.; Grosse-Kunstleve, R. W.; Adams, P. D.; Winn, M. D.; Storoni, L. C.; Read, R. J. Phaser crystallographic software. *J. Appl. Crystallogr.* **2007**, *40* (4), 658−674.

(35) Vagin, A. A.; Steiner, R. A.; Lebedev, A. A.; Potterton, L.; McNicholas, S.; Long, F.; Murshudov, G. N. REFMAC5 dictionary: organization of prior chemical knowledge and guidelines for its use. *Acta Crystallogr., Sect. D: Biol. Crystallogr.* **2004**, *60* (12), 2184−2195.

(36) Emsley, P.; Lohkamp, B.; Scott, W. G.; Cowtan, K. Features and development of Coot. *Acta Crystallogr., Sect. D: Biol. Crystallogr.* **2010**, *66* (4), 486−501.

(37) Murshudov, G. N.; Skubák, P.; Lebedev, A. A.; Pannu, N. S.; Steiner, R. A.; Nicholls, R. A.; Winn, M. D.; Long, F.; Vagin, A. A. REFMAC5 for the refinement of macromolecular crystal structures. *Acta Crystallogr., Sect. D: Biol. Crystallogr.* **2011**, *67* (4), 355−367.

(38) Nicholls, R. A.; Long, F.; Murshudov, G. N. Low-resolution refinement tools in REFMAC5. *Acta Crystallogr., Sect. D: Biol. Crystallogr.* **2012**, *68* (4), 404−417.

(39) Murshudov, G. N.; Vagin, A. A.; Dodson, E. J. Refinement of macromolecular structures by the maximum-likelihood method. *Acta Crystallogr., Sect. D: Biol. Crystallogr.* **1997**, *53* (3), 240−255.

(40) Winn, M. D.; Murshudov, G. N.; Papiz, M. Z. Macromolecular TLS refinement in REFMAC at moderate resolutions. *Methods Enzymol.* **2003**, *374*, 300−321.

(41) van Aalten, D. M.; Bywater, R.; Findlay, J. B.; Hendlich, M.; Hooft, R. W.; Vriend, G. PRODRG, a program for generating molecular topologies and unique molecular descriptors from coordinates of small molecules. *J. Comput. Aided Mol. Des.* **1996**, *10* (3), 255−262.

(42) Konermann, L. Addressing a Common Misconception: Ammonium Acetate as Neutral pH ″Buffer″ for Native Electrospray Mass Spectrometry. *J. Am. Soc. Mass Spectrom.* **2017**, *28* (9), 1827−1835.

(43) Polasky, D. A.; Dixit, S. M.; Fantin, S. M.; Ruotolo, B. T. CIUSuite 2: Next-Generation Software for the Analysis of Gas-Phase Protein Unfolding Data. *Anal. Chem.* **2019**, *91* (4), 3147−3155.

(44) May, J. C.; Jurneczko, E.; Stow, S. M.; Kratochvil, I.; Kalkhof, S.; McLean, J. A. Conformational Landscapes of Ubiquitin, Cytochrome c, and Myoglobin: Uniform Field Ion Mobility Measurements in Helium and Nitrogen Drift Gas. *Int. J. Mass Spectrom.* **2018**, *427*, 79−90.

(45) Ruotolo, B. T.; Benesch, J. L. P.; Sandercock, A. M.; Hyung, S.-J.; Robinson, C. V. Ion mobility-mass spectrometry analysis of large protein complexes. *Nat. Protoc.* **2008**, *3* (7), 1139−1152.